A peer-reviewed version of this preprint was published in PeerJ on 19 December 2019.

View the peer-reviewed version (peerj.com/articles/8112), which is the preferred citable publication unless you specifically need to cite this preprint.

Santaella BL, Tseng ZJ. 2019. Hole in One: an element reduction approach to modeling bone porosity in finite element analysis. PeerJ 7:e8112 https://doi.org/10.7717/peerj.8112

Hole in One: an element reduction approach to modeling bone porosity in finite element analysis

Beatriz L Santaella [Corresp., 1], **Z. Jack Tseng** [1]

[1] Department of Pathology and Anatomical Sciences, Jacobs School of Medicine and Biomedical Sciences, State University of New York at Buffalo, Buffalo, New York, United States

Corresponding Author: Beatriz L Santaella
Email address: bsantaella@outlook.com

Finite element analysis has been an increasingly widely used tool in many different science and engineering fields over the last decade. In the biological sciences, there are many examples of its use in areas as paleontology and functional morphology. Despite this common use, the modeling of porous structures such as trabecular bone remains a key issue because of the difficulty of meshing such highly complex geometries during the modeling process. A common practice is to mathematically adjust the boundary conditions (i.e. model material properties) of whole or portions of models that represent trabecular bone. In this study we aimed to demonstrate that a physical, element reduction approach constitutes a valid protocol to this problem in addition to the mathematical approach. We tested a new element reduction modeling script on five exemplar trabecular geometry models of carnivoran temporomandibular joints, and compared stress results of both physical and mathematical approaches to trabecular modeling to models incorporating actual trabecular geometry. Simulation results indicate that that the physical, element reduction approach generally outperformed the mathematical approach. Physical changes in the internal structure of experimental cylindrical models had a major influence on the recorded stress values throughout the model, and more closely approximates values obtained in models containing actual trabecular geometry than solid models with modified trabecular material properties. Therefore, we conclude that for modeling trabecular bone in finite element simulations, maintaining or mimicking the internal porosity of a trabecular structure is recommended as a fast and effective method in place of, or alongside, modification of material property parameters to better approximate trabecular bone behavior observed in models containing actual trabecular geometry.

Hole in One: an element reduction approach to modeling bone porosity in finite element analysis

Beatriz L. Santaella[1], Z. Jack Tseng[1]

[1]Computational Cell Biology, Anatomy, and Pathology Program, Department of Pathology and Anatomical Sciences, Jacobs School of Medicine and Biomedical Sciences, State University of New York, Buffalo, New York 14203, U.S.A.

Corresponding Author:
Beatriz L. Santaella

Jacobs School of Medicine and Biomedical Sciences, 955 Main St.
Buffalo, NY 14203, U.S.A.
Email address: bsantaella@outlook.com

PeerJ Preprints | https://doi.org/10.7287/peerj.preprints.27909v1 | CC BY 4.0 Open Access | rec: 19 Aug 2019, publ: 19 Aug 2019

Abstract

Finite element analysis has been an increasingly widely used tool in many different science and engineering fields over the last decade. In the biological sciences, there are many examples of its use in areas as paleontology and functional morphology. Despite this common use, the modeling of porous structures such as trabecular bone remains a key issue because of the difficulty of meshing such highly complex geometries during the modeling process. A common practice is to mathematically adjust the boundary conditions (i.e. model material properties) of whole or portions of models that represent trabecular bone. In this study we aimed to demonstrate that a physical, element reduction approach constitutes a valid protocol to this problem in addition to the mathematical approach. We tested a new element reduction modeling script on five exemplar trabecular geometry models of carnivoran temporomandibular joints, and compared stress results of both physical and mathematical approaches to trabecular modeling to models incorporating actual trabecular geometry. Simulation results indicate that that the physical, element reduction approach generally outperformed the mathematical approach. Physical changes in the internal structure of experimental cylindrical models had a major influence on the recorded stress values throughout the model, and more closely approximates values obtained in models containing actual trabecular geometry than solid models with modified trabecular material properties. Therefore, we conclude that for modeling trabecular bone in finite element simulations, maintaining or mimicking the internal porosity of a trabecular structure is recommended as a fast and effective method in place of, or alongside, modification of material property parameters to better approximate trabecular bone behavior observed in models containing actual trabecular geometry.

Introduction

Finite element analysis (FEA) is a continuum mechanics-based technique originally conceived and used in the engineering design process to predict the behavior (i.e. response) of structures to prescribed loading conditions using discretized representations of those structures, thereby enabling the design of these systems to be optimized mathematically with minimum physical prototyping and testing (Dumont et al., 2009; Zienkiewicz and Taylor, 2000). With advances in computer software packages that allow a seamless connection of FEA to CAD and image data based modeling, the simulation method has also been applied to functional morphological research in organismal biology, including extinct organisms (Ross, 2005; Rayfield, 2007; Bright, 2014). FEA of feeding mechanics of living and extinct vertebrates have been used in comparative functional morphology for more than a decade (Rayfield, 2005; Alexander, 2006; Barrett and Rayfield, 2006; McHenry et al., 2006; Thomasson et al., 2007), and the method also has been applied in studies in other organismal systems such as insect flight and

mechanoreception (Combes and Daniel, 2003; Dechant et al., 2006; Wootton, 2003), and plant biomechanics (Fourcaud and Lac, 2003; Niklas, 1999).

The pushing of the boundary for FEA and better modeling of bone structures have been continuous for the last decade or so to better understand skeletal form and function (Rayfield, 2007; Bourke et al., 2008; Wroe et al., 2008; Strait et al., 2010). Still, porous structures like trabecular bone and other complex biological geometries remain problematic in FE modeling given their internal complexity, and the conversion from 2D to 3D of intricate structures that frequently generate errors in elemental overlaps and highly skewed elemental shapes in small anatomical regions. Based on our experience working with bone meshes, biological structures with a high amount of trabecular bone or porous components have higher chances of meshing errors in the FE solid meshing process. When in the presence of this type of porous structures it is common to avoid the complexity of creating an accurate trabecular network by modeling entire models as homogeneous cortical bone and ignoring trabecular geometry, and/or changing the material properties in different element groups within a model to represent cortical versus trabecular bones (Strait et al., 2005, 2009; Wroe, 2008; Attard et al., 2011; Chamoli and Wroe, 2011). This general simplification approach is used in most comparative studies using FEA that incorporate trabecular morphology, even though it has been demonstrated that trabecular structures have a very important role in the performance of a mesh when using FEA (Parr et al., 2013).

Our objective in this study is to test an alternative, mechanical approach to trabecular bone modeling as a viable solution in addition to mathematical approaches (i.e., changing the material properties of solid models). Potential solutions to accommodate trabecular morphology in finite element modeling that can bypass time-consuming and scan resolution-dependent micro-modeling of trabecular structures are desired. We aim to test the hypothesis that percentage porosity adjustments in solid finite element meshes will generate simulation results comparable or closer to those using actual trabecular morphology, compared to solid models using only modified material property parameter values to simulate trabecular bone behavior.

Materials and Methods

We used 5 species samples to test a finite element reduction approach to trabecular bone modeling relative to actual trabecular structural models. Each species-specific test sample is represented by three types of experimental cylindrical models: one control cylinder (CC); one "physically modified" cylinder (PC); and one "material modified" cylinder (MC).

Control group cylinders

The spongy bone cylinder core meshes were taken from (Wysocki and Tseng, 2018), based on scans of skull specimens from the American Museum of Natural History (*Arctonyx collaris*;

Bassariscus astutus; *Enhydra lutris*; *Mellivora capensis*; *Vulpes vulpes*) (see Table S1 for scanning parameters). We emphasize that this is not a full-scale comparative analysis; the species were selected based on the relative fill volume range (the amount of space within a predefined digital cylinder sample of trabecular network within the temporomandibular joints of each species that is bone) (Wysocki and Tseng, 2018), ensuring testing of each trabecular material modification method over a relatively wide range of naturally occurring variations in trabecular density. The range of relative fill volumes span from 7.8% in *Mellivora capensis* to 46.6% in *Bassariscus astutus*. These specimen-derived cylinders correspond to a 'control group' to serve as a reference for PC and MC changes in values of von Misses stress. Von Mises stress is a good predictor of failure under ductile fracture, and an appropriate metric for comparing the relative strength of models of bones (Dumont et al., 2009).

Full cylinders corresponding to the maximum, solid volumes possible for the virtual cylindrical cores used in Wysocki and Tseng (2018) were designed in Geomagic Wrap 2017.0.1.19 (3D Systems, Rock Hill, South Carolina) with a 10mm height and 5mm diameter. Ten cylinders were created, five to be modified by physical element reduction to increase porosity, and the other five to be modified in their material properties but not physical geometry (i.e. they remain solid cylinders). When finished, the cylinders were exported as binary stereolithographic files (.stl). These models serve as input for further processing in the finite element simulation software.

Material modified cylinder group

We defined the material properties to apply in all the meshes in the CC and PC experimental groups (Young's Modulus: 20 GPa and Poisson's Ratio: 0.3). For the MC group, the Young's Modulus is adjusted within a range (from 7 GPa to 22 GPa) that is linearly proportional to the density values of the control cylinder (actual species trabecular geometry) for that experimental group's relative fill volume. Relative fill volume (mm^3) was calculated using the species-derived 3D model that served as the standard (Wysocki and Tseng., 2018). The remaining boundary conditions for the MC group were set up as in the CC group.

Physically modified cylinder group

A set of the solid meshed cylinders were post-processed using a custom script built in R 3.5.1 (R Foundation for Statistical Computing, Vienna, Austria) that created an induced porosity into cylinder models by randomized solid element removal (https://github.com/BeaSantaella/Hole-in-One.git). After importing a solid mesh file from Strand7 into R, then designating a user-defined amount of tetrahedral deletion (as a percentage), the script will randomly go through all the brick elements (which form the structure modeled, and are formed by individual, four-noded tetrahedral elements) and remove the designated percentage from the model. Each tetrahedral element can be randomly selected for removal only once; in other words, randomized selection

of elements for removal is done without replacement. the script output is a text file (.txt) in Strand7 format.

Each script was assigned a certain percentage of deletion based on the relative fill volume of their corresponding CC (26.1% for *Arctonyx collaris;* 46.6% for *Bassariscus astutus*; 16.5% for *Enhydra lutris*; 7.8% for *Mellivora capensis*; 35.8% for *Vulpes vulpes*).

Element Reduction Script Verification Analyses

Before comparing PC models to the CC group or MC group, we tested an additional set of 5 models with the intention to ascertain the internal consistency of the script (whether consistent results can be obtained using the random element deletion algorithm proposed). If significant differences in magnitude of the stress values are present in script-generated models across different replicates, the script would not represent a true randomized approach to element reduction. If the effects of the script are random, the variability in the results for all 5 cases should be within comparable ranges of variation. Some variability is expected because the script is based on a random pattern, as a consequence, some arbitrary associations that affect stress values may occur. Overall, our assumption is that replication of porosity in trabecular structures by random reduction of solid element would results in replication of overall trabecular mechanical behavior.

We applied the same script, set at 16.5% volume deletion, to five otherwise identical solid cylinder models. We chose 16.5% deletion as a middle-value through our tested range (7.8% to 46.6%). The rest of the parameter values, such as material properties (being Young Modulus: 20 GPa and Poisson's Ratio: 0.3), the amount of force applied (1000N), nodes retrained (four nodes, at the end of a cross-section, at the bottom of the cylinder), and the area of application all remained identical (see description above). All the points sampled were identical through all of the five cylinders (Fig.1).

Combined PC and MC model group

In order to assess to joint efficacy of introducing both physical porosity and modification of material property parameters, another set of models were created. They present the same percentage of deletion to corresponding PC models, but their material properties were also adjusted to their corresponding MC models.

Model Simulation Parameters

We use Finite Element Analysis (FEA) software Strand7 2.4.6 (G1D Computing Pty, Sydney, Australia) to solid mesh the surface cylinder models generated in Geomagic Wrap. In FEA the physical domain geometry is approximated by a mesh of simple polyhedral shapes called ‘finite elements’, connected together at ‘nodes’, which are the vertices of the polyhedrons (Dumont et al., 2009). These polyhedrons also are known as "bricks" in Strand7 and they form the shape of

the cylinders from the original triangles (the cylindrical surface meshes generated in Geomagic Wrap). A mesh formed by bricks is considered a solid mesh, the mesh type used for finite element analysis in the majority of 3D comparative functional morphology studies.

We applied an arbitrary, 1000N of force over the nodes on the entire top surface of all cylinder models and recorded nodal stress values (von Mises stress) at four transects in each model. We sampled a total 40 points along the surface of the cylinders (from top to bottom, 10 sampling points per transect). The stress values collected from these nodal transects are used to compare the CC, PC, MC, and PC+MC experimental groups (Fig.1). All analyses were linear static. Model files for all analyses conducted are available for download at Zendodo (https://doi.org/10.5281/zenodo.3344501).

Results

Our results show that physically modified cylinder replicates, assigned the same specific settings, have uniform outputs (Fig. 2, Table S2). There was only a small problematic region, located at the bottom (points 8 to 10) of cylinder IV. Because there are no differences between the cylinders beside the random arrangements that the script may have produced, the higher stress values on the nodes correspond to a more significant deletion at the sampled area. The higher deletion around that area would affect how the applied force is transmitted and distributed in that location, and it will extend influence to contiguous areas (as subsequent points show higher stress values). This inconsistency should be diluted due to the number of sample nodes used for the final test (40 per cylinder).

There is a better overall performance of the PC in comparison with MC when referring to the CC. In the first two experimental groups (Fig. 3A-3B, Tables S3-S4, S8-S9, S13-S14), we see a consistent performance of the PC. We can see a slightly more accurate trend in PC (it underestimates in certain regions, but replicates peaks and valleys, in other words, replicates the general trend). The bottom section of the PC cylinders has a more accurate performance than the MC. MCs in both figures have a linear trend with minimum stress changes.

Nevertheless, in experimental group 3 (Fig. 3C, Tables S5, S10, S15), PC seemed to be unable to correctly replicate both trend and stress values of the control group. On the other hand, for experimental group 4 (Fig. 3D, Tables S6, S11, S16), the PC seems to perform well in some of the points (same stress values or off by less than 10 MPa). Except at the beginning and the end (where higher variability may be present, close to the area of force application and nodal restraints). The nature of the trend by CC is correctly replicated in both PC and MC.

In experimental group 5 (Fig. 3E, Tables S7, S12, S17), the differences in stress values seem to be consistent with what we observe in groups 1 and 2 (Fig. 3A and Fig. 3B). PC replicates the

overall CC trend but it is off by 60 to 80 MPa, especially at the core. MC shows a less accurate trend, with a more linear pattern, and no resemblance to the CC trend is observed.

As seen in all experimental groups (Fig. 3A-3D, Tables S18-S21) the combined PC+MC approach presents the same stress values as the PC group results. The differences are statistically indistinguishable between PC and PC+MC results.

Discussion

Our aim in this study is to demonstrate an element reduction approach to modeling trabecular networks. We tested the hypothesis that, even if they are not 100% replicates of trabecular bone models, porous FE models can at least behave in a comparable way, and provide a closer approximation of mechanical behavior than only modifying overall material property parameters of solid models. Our results indicate that an element reduction approach to modeling bone porosity produced stress magnitudes that are generally closer to values generated from models containing actual trabecular bone geometry, compared to only modifying material properties to simulate bone porosity (Fig. 4).

Bone tissue can behave as a homogeneous material on a microscale (Muller, 2009) with both individual trabeculae and compact bone having similar material properties (Rho et al., 1993). Therefore, changing material properties to differentiate compact versus trabecular bone may not adequately replicate bone behavior in FE simulations. Taking into consideration that we adjusted bone porosity changes based on the internal density of the cylinder, PC models did better replicating the stress values of the control group than MC models (see Fig. 3A, Fig. 3B). Accordingly, the mathematical approach (change in the material properties) is a less effective way to approximate model mechanical behavior than physically reducing the element density of solid mesh models via the randomization approach tested in this study. In addition, models with both physically introduced porosity and material property parameter changes combined behaved similarly to the models with only introduced porosity, suggesting the dominant role of element reduction in dictating mechanical behavior of the cylinder models.

It is remarkable that even without a cover of cortical bone (or a thick layer that might homogenize the values at the nodal transect regions) the mechanical modeling approach still has a certain consistency (results are similar in all four experimental groups for PC+MC models). Based on our results, the ability of PC models to approximate the control group models is best in moderate density models. As shown in Fig. 3E, the peaks in the CC model are replicated more closely by PC, whereas MC trends show a low-sensitivity trajectory. Indicating that the overall performance of MCs is less accurate than observed for data in the PC group.

It is also quite clear that material properties modified cylinders behave as a stiffer material than the other two groups. The von Mises stress values, which reflect the likeliness of a certain structure to fail, are significantly lower in MC. This stiffness, or lack of it, may be related to the internal network influence on the overall performance (Parr et al., 2013).

It is worth pointing out that the peaks in the plot (for the control group) might be explained by how close the sampled node was to a physical hole or opening on the model surface (in other words, adjacent to an internal porous network). The nodal values may be influenced by elevated stress values associated with such porosity. Thus, creating a cover layer of plate elements, then sampling from that surface, could be a solution to account for the source of that possible noise. This could be considered in further studies, but our goal for this first study was to compare relative performances between the mechanical approach and the mathematical approach (PC vs MC); rather than specifically creating a protocol to mimic actual bone.

Lastly, we note that the element reduction script generated models with holes in a random pattern, whereas the actual species trabecular geometries contain holes surrounding a network of bony struts. As a consequence, PC models are more homogeneous in how they distribute forces. In other words, when compared to the CC group, the PC models perform as a stiffer material. This is probably related to their lack of internal heterogeneity in arrangements or concentration of large pores/bony struts that may not be represented by the mechanical modeling approach. This is another key factor to consider in future research into improving accuracy of trabecular bone modeling in FE simulations.

Conclusions

We demonstrated that an element reduction approach to modeling trabecular structure could more closely simulate behavior of trabecular geometry compared to changing material properties in solid models. We suggest that, unless the complex geometry of trabecular bone is precisely accounted for during the model building process, researchers should first consider modeling the porosity of the material instead of, or in addition to, changing material properties. This recommendation is supported by our findings that indicate physical internal porosity generation better approximates mechanical performance of trabecular structures both as a standalone protocol or in combination with material property changes, compared to material property changes alone. Therefore, we recommend taking into account bone porosity in such a physical manner in biomechanical modeling of complex trabecular bone geometries in comparative functional morphological studies, as a fast and effective way to approximate trabecular geometry.

Acknowledgments

We thank M. Wysocki for providing cylindrical models of the carnivoran species tested in this study. B. Santaella was funded by a research scholarship from the Functional Anatomy and Vertebrate Evolution Laboratory. B. Santaella thanks committee members J. Liu and S. Doyle for their time and advice.

References

Alexander, R.M., 2006. Dinosaur biomechanics. Proc. Roy. Soc. Biol. Sci. Ser. B 273,1849–1855.

Attard, M.R.G., Chamoli, U., Ferrara, T.L., Rogers, T.L., Wroe, S., 2011. Skull mechanics and implications for feeding behaviour in a large marsupial carnivore guild: the thylacine, Tasmanian devil and spotted-tailed quoll. Journal of Zoology 285 (4), 292–300.

Barrett, P.M., Rayfield, E.J., 2006. Ecological and evolutionary implications of dinosaur feeding behaviour. Trends Ecol. Evol. 21, 217–224.

Bourke, J., Wroe, S., Moreno, K., McHenry, C.R., Clausen, P.D., 2008. Effects of gape and tooth position on bite force in the dingo (Canis lupus dingo) using a 3-Dfinite element approach. PLoS One 3, 1–5.

Bright, J. A., 2014. A review of paleontological finite element models and their validity. Journal of Paleontology, 88(4), 760-769.

Chamoli, U., Wroe, S., 2011. Allometry in the distribution of material properties and geometry of the felid skull: why larger species may need to change and how they may achieve it. Journal of Theoretical Biology 283 (1), 217–226.

Combes, S.A., Daniel, T.L., 2003. Into thin air: contributions of aerodynamic and inertial-elastic forces to wing bending in the hawkmoth Manduca sexta. J. Exp.Biol. 206, 2999–3006.

Dechant, H.E., Hossl, B., Rammerstorfer, F.G., Barth, F.G., 2006. Arthropodmechanoreceptive hairs: modeling the directionality of the joint. J. Comp. Physiol. A 192, 1271–1278.

Dumont, E. R., Grosse, I. R., & Slater, G. J., 2009. Requirements for comparing the performance of finite element models of biological structures. Journal of theoretical biology, 256(1), 96-103.

Fourcaud, T., Lac, P., 2003. Numerical modelling of shape regulation and growth stresses in trees I. An incremental static finite element formulation. Trees 19,23–30.

McHenry, C.R., Clausen, P.D., Daniel, W.J.T., Meers, M.B., Pendharkar, A., 2006.Biomechanics of the rostrum in crocodilians: a comparative analysis using finite-element modeling. The Anat. Rec.: Adv. Integr. Anat. Evol. Biol. 288,827–849.

Niklas, K.J., 1999. A mechanical perspective on foliage leaf form and function. NewPhytol. 143, 19–31.

Parr, W., Chamoli, U., Jones, A., Walsh, W., & Wroe, S., 2013. Finite element micro-modelling of a human ankle bone reveals the importance of the trabecular network to mechanical performance: new methods for the generation and comparison of 3D models. Journal of biomechanics, 46(1), 200-205.

Rayfield, E. J., 2005. Aspects of comparative cranial mechanics in the theropod dinosaurs Coelophysis, Allosaurus and Tyrannosaurus. Zoological Journal of the Linnean Society, 144(3), 309-316.

Rayfield, E.J., 2007. Finite element analysis and understanding the biomechanics and evolution of living and fossil organisms. Annual Review of Earth and Planetary Sciences 35, 541–576.

Ross CF. 2005. Finite element analysis in vertebrate biomechanics. Anat Rec A Discov Mol Cell Evol Biol 283: 253–258.

Strait, D., Wang, Q., Dechow, P.C., Ross, C.F., Richmond, B.G., Spencer, M.A., Patel,B.A., 2005. Modelling elastic properties in finite element analysis: how much precision is needed to produce an accurate model? The Anatomical Record Part A 283A, 275–287.

Strait, D.S., Weber, G.W., Neubauer, S., Chalk, J., Richmond, B.G., Lucas, P.W.,Spencer, M.A., Schrein, C., Dechow, P.C., Ross, C.F., Grosse, I.R., Wright, B.W.,Constantino, P., Wood, B.A., Lawn, B., Hylander, W.L., Wang, Q., Byron, C., Slice, D.E., Smith, A.L., 2009. The feeding biomechanics and dietary ecology of Australopithecus africanus. Proceedings of the National Academy of Sciences of the United States of America 106, 2124–2129.

Strait, D.S., Grosse, I.R., Dechow, P.C., Smith, A.L., Wang, Q., Weber, G.W., Neubauer,S., Slice, D.E., Chalk, J., Richmond, B.G., Lucas, P.W., Spencer, M.A., Schrein, C.,Wright, B.W., Byron, C., Ross, C.F., 2010. The structural rigidity of the cranium of Australopithecus africanus: implications for diet, dietary adaptations, and the allometry of feeding biomechanics. Anatomical Record: Advances in Integrative Anatomy and Evolutionary Biology 293, 583–593.

Thomassen, H.A., Gea, S., Maas, S., Bout, R.G., Dirckx, J.J.J., Decraemer, W.F., Povel,G.D.E., 2007. Do Swiftlets have an ear for echolocation? The functional morphology of Swiftlets' middle ears. Hearing Res. 225, 25–37.

Tseng, Z. J., & Wang, X., 2010. Cranial functional morphology of fossil dogs and adaptation for durophagy in Borophagus and Epicyon (Carnivora, Mammalia). Journal of Morphology, 271(11), 1386-1398.

Wootton, R., 2003. Finite element analysis, or bent cardboard? Approaches to modelling insect wings. Antenna 27, 310–313.

Wroe, S., Huber, D.R., Lowry, M., McHenry, C., Moreno, K., Clausen, P., Ferrara, T.L.,Cunningham, E., Dean, M.N., Summers, A.P., 2008. Three-dimensional computer analysis of white shark jaw mechanics: how hard can a great white bite? Journal of Zoology 276, 336–342.

Wroe, S., 2008. Cranial mechanics compared in extinct marsupial and extant African lions using a finite-element approach. Journal of Zoology 274, 332–339.

Wysocki, M. A., & Tseng, Z. J. 2018. Allometry predicts trabecular bone structural properties in the carnivoran jaw joint. PloS one, 13(8), e0202824.

Zienkiewicz, O.C., & Taylor, R.L., 2000. Finite Element Method: vol. 1. The Basis.Butterworth-Heinemann, Oxford.

Figure 1(on next page)

Locations of boundary conditions on the cylinder models (fix nodes; force and sample transect).

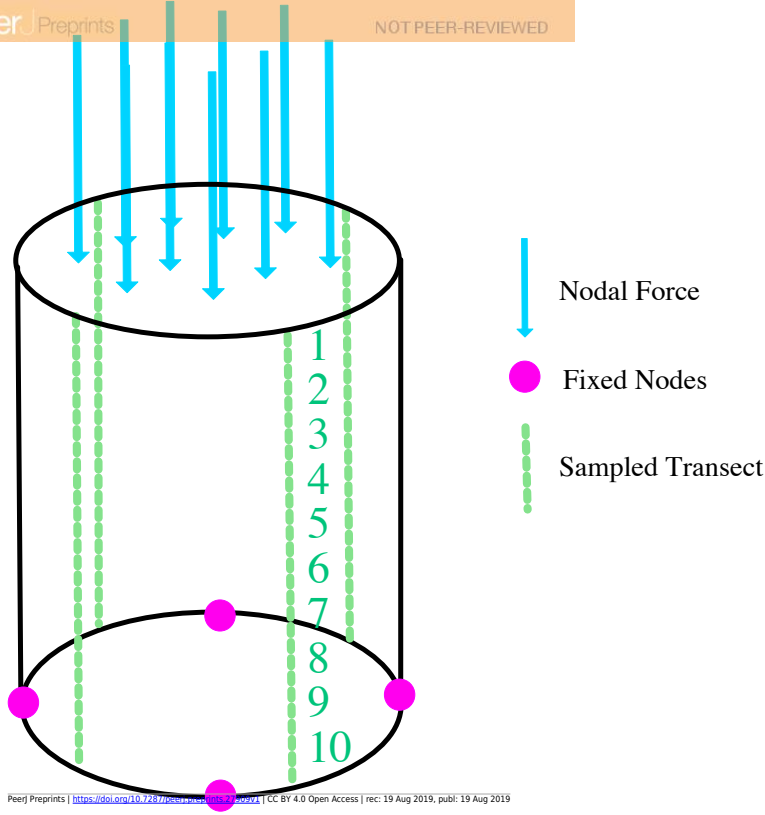

PeerJ Preprints | https://doi.org/10.7287/peerj.preprints.27907v1 | CC BY 4.0 Open Access | rec: 19 Aug 2019, publ: 19 Aug 2019

Figure 2(on next page)

Element reduction script performance consistency.

Sampled nodes represent 10 equidistant points along data transects where von Mises stress values were recorded (as described in Table S2). The different cylinder model replicates are labeled from I to V.

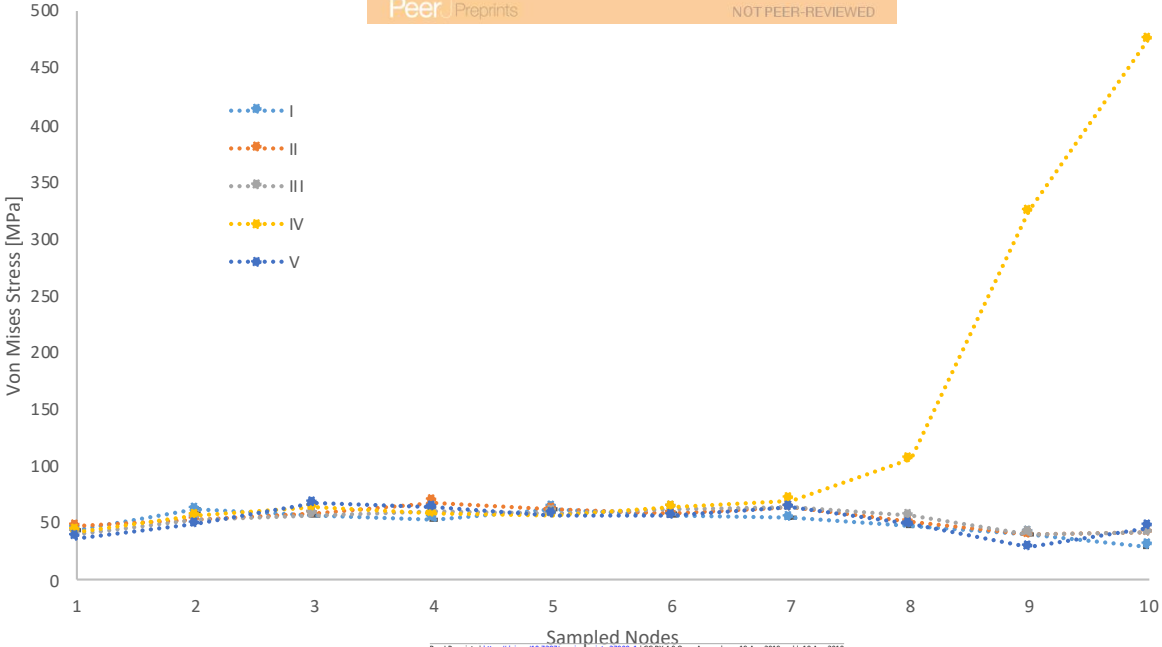

PeerJ Preprints | https://doi.org/10.7287/peerj.preprints.27909v1 | CC BY 4.0 Open Access | rec: 19 Aug 2019, publ: 19 Aug 2019

Figure 3(on next page)

Experimental groups 1 to 5.

On the x-axis, we display 10 points used to collect the data (point 1 top, point 10 bottom). On the y-axis, we show Von Mises stress values. The blue line corresponds with the CC; the orange line corresponds with the PC; the grey line corresponds with MC; the green line corresponds with PC+MC. A (CC: *Arctonyx*; PC: 26.1%; MC; 16GPa), B (CC: *Bassariscus*; PC: 46.6%; MC; 7GPa), B (CC: *Enhydra*; PC: 16.5%; MC; 20GPa), D (CC: *Mellivora*; PC: 7.8%; MC; 22GPa), E (CC: *Vulpes*; PC: 35.8%; MC; 10GPa). Error bars represent the confident intervals of the mean at 95 percent. (See Tables S3 to S21)

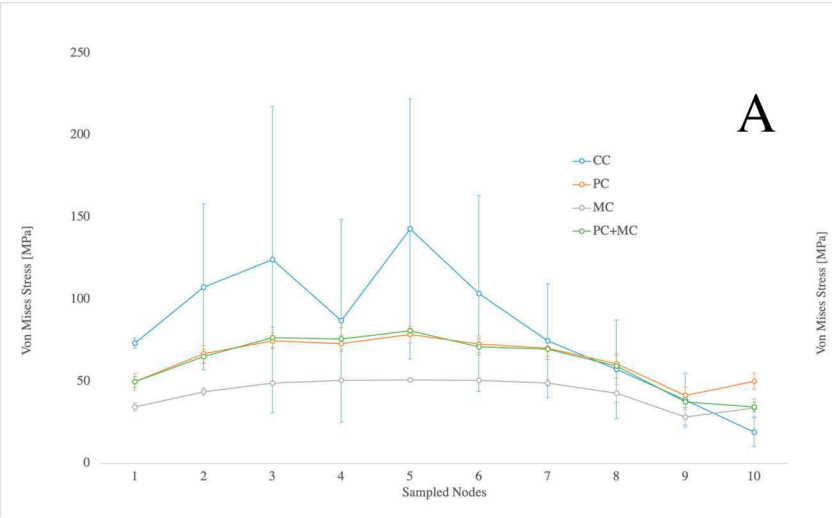

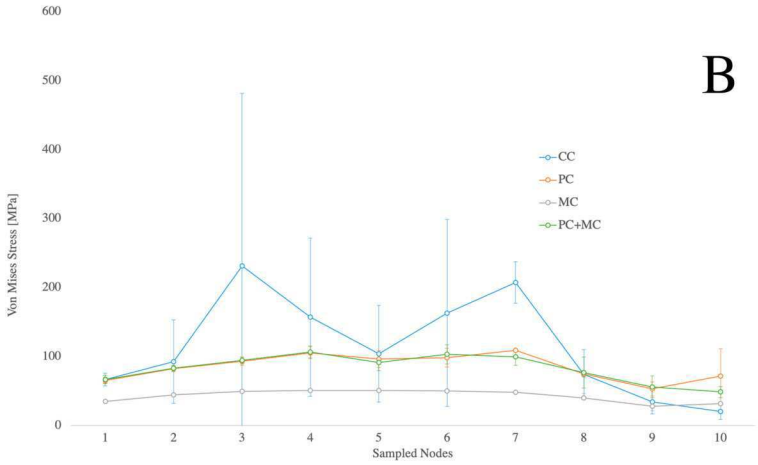

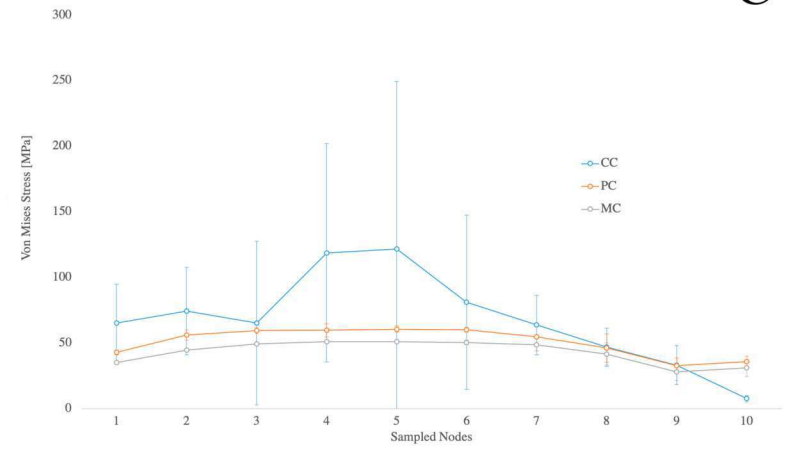

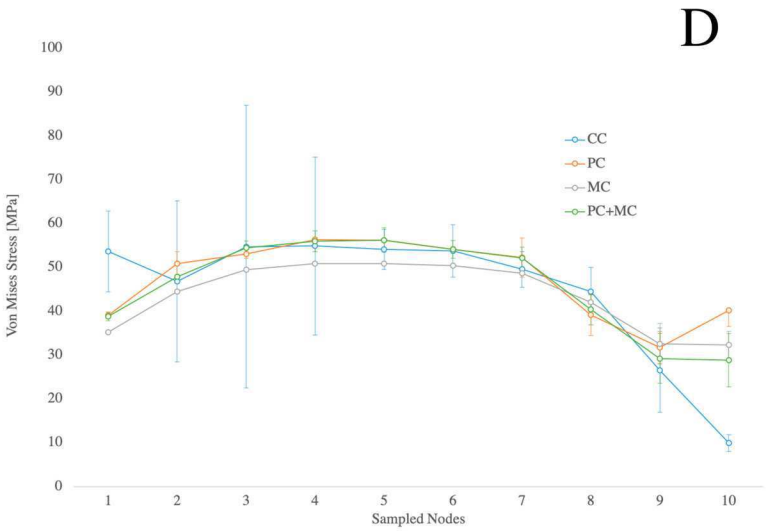

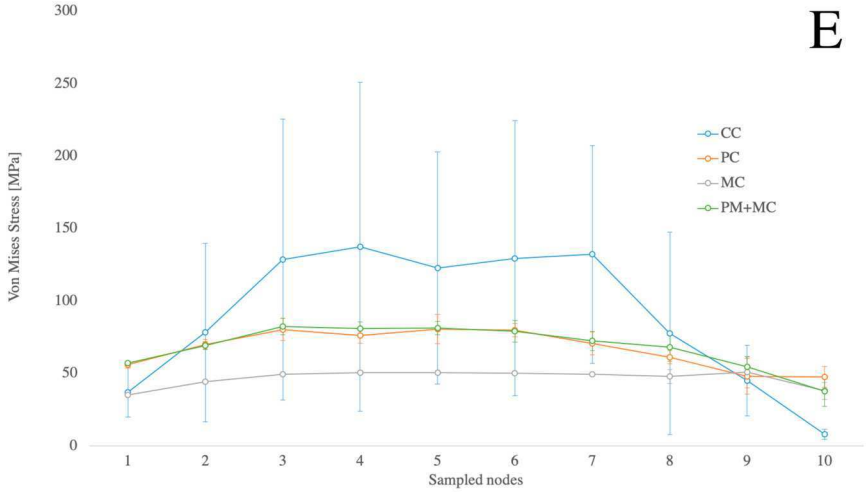

Figure 4

Visualization of von Mises stress in the cylinders.

Vertically the image is separated into three sections (CC, PC, and MC); horizontally we show five levels one per experimental group.